iScience

CellPress
OPEN ACCESS

Article

Catchment-wide flooding significantly altered microplastics organization in the hydro-fluctuation belt of the reservoir

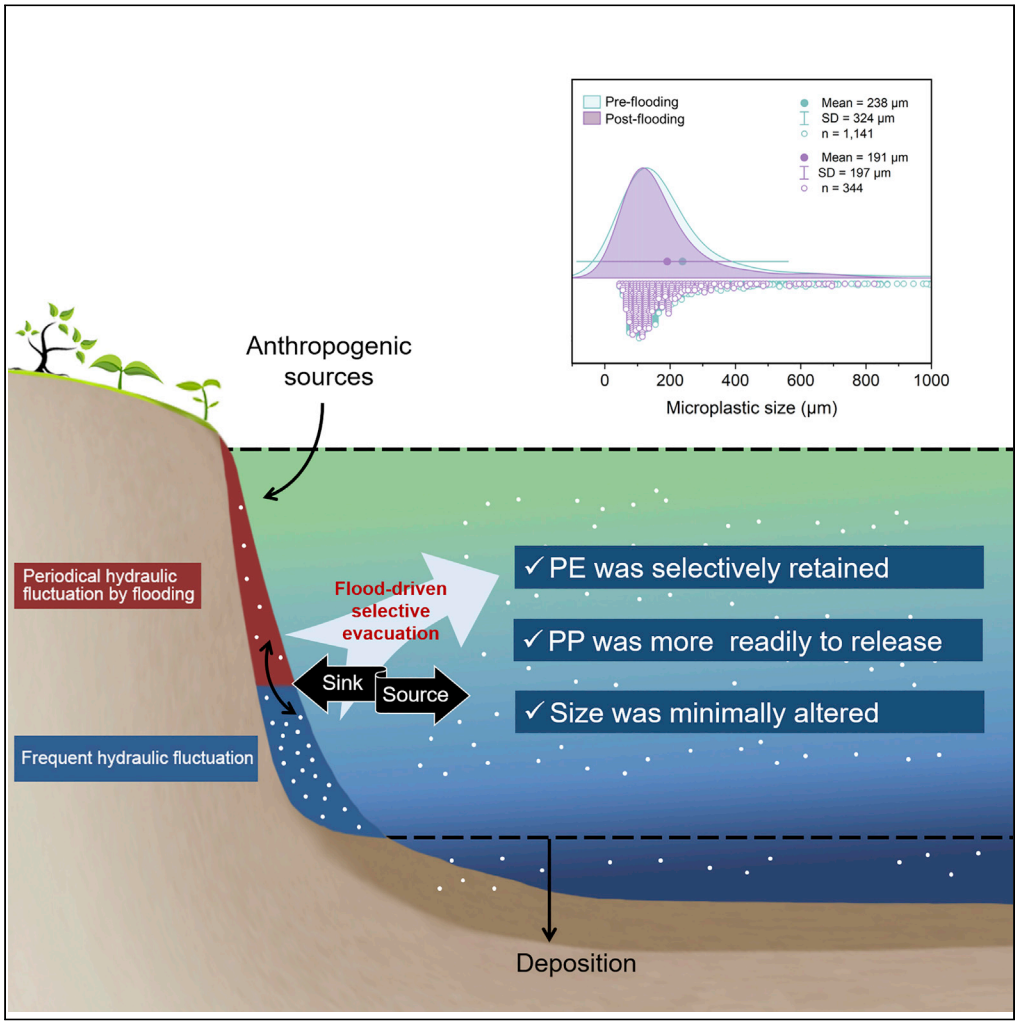

Yalan Chen, Bo Gao, Dongyu Xu, Ke Sun, Yanyan Li

gaobo@iwhr.com

Highlights

Microplastics were detected across all sites in hydro-fluctuation belt (HFB) soil

Flooding efficiently reduced local microplastics in HFB soil

Catastrophic flooding induced selective retention of microplastics in HFB soil

HFB soil was a significant source of microplastics in the reservoir basin

Chen et al., iScience *25*, 104401
June 17, 2022
https://doi.org/10.1016/j.isci.2022.104401

iScience

CellPress
OPEN ACCESS

Article

Catchment-wide flooding significantly altered microplastics organization in the hydro-fluctuation belt of the reservoir

Yalan Chen,[1,2] Bo Gao,[1,3,*] Dongyu Xu,[1] Ke Sun,[2] and Yanyan Li[1]

SUMMARY

Hydro-fluctuation belt (HFB) is the most sensitive area of a large reservoir. This research aimed to identify the impact of catastrophic flooding on the local microplastics organization in the HFB soil of the Three Gorges Reservoir, the largest reservoir in China. We found that the catchment-wide flooding efficiently alleviated the local microplastics abundance from 7,633 to 4,875 items/kg (from 44 to 18 mg/kg) but added to the pollution risk in the reservoir body. After flooding, the overall size distribution of local microplastics was minimally altered. Interestingly, the preferential retention of the small-sized polyethylene was found in HFB after flooding. Approximately 5.0×10^{14} items (~2,360 tons) of microplastics were evacuated into the reservoir, equivalent to 15.8 wt% of the plastic flux of the Yangtze River into the ocean. We observed that HFB is a significant source of local microplastics in reservoir, and the long-term source–sink transformation mechanism in the HFB should be further investigated.

INTRODUCTION

Nowadays, plastics are widely used in daily life owing to their durability and low cost. According to the latest statistics from PlasticEurope, the global plastic production in 2019 reached 359 million tons (PlasticEurope, 2020). However, only a small proportion (about 6–26%) of this amount will be recycled (Alimi et al., 2018). Improper disposal resulted in the accumulation of over 4.9 billion tons of plastic waste in the environment (Geyer et al., 2017). The plastic waste will naturally weather and break into microplastics (<5 mm), which are more hazardous to the environment. Owing to their hydrophobicity and mobility, microplastics can act as an efficient vector for environmental pollutants and affect their transport and secondary release (Koelmans et al., 2016). Meanwhile, aquatic and terrestrial organisms can also be affected by accidental ingestion of smaller microplastics (Jin et al., 2019). Moreover, microplastics can alter the ambient microbial community, thereafter influencing the natural carbon and nitrogen cycle of sediments (Seeley et al., 2020). As plastics are likely to be widely used for many years to come owing to the lack of alternative products, information about the occurrence and fate of microplastics is of considerable urgency for evaluating their ecological risks.

The Three Gorges Dam is the largest hydropower plant worldwide. Originally constructed for managing flood discharge, the dam has significantly modified its surrounding hydrological regimes, converting vast upstream regions into a lentic reservoir (the Three Gorges Reservoir (TGR)) (Nilsson et al., 2005). The anti-seasonal fluctuation of water levels in the TGR region has formed a unique area known as the hydro-fluctuation belt (HFB). The HFB undergoes periodic exposure and is one of the most sensitive areas in the TGR. The special hydrodynamic conditions of the TGR may lead to a highly dynamic role switching of the HFB as a source or sink of microplastics (Woodward et al., 2021; Zhang et al., 2019). The occurrence of microplastics at a given location in HFB reflected a current state of microplastics contamination after repeated hydraulic sorting over time (Pabortsava and Lampitt, 2020). When the water level increases, microplastics present in the surface and subsurface water may accumulate in the riparian soil that comes in contact with the water; meanwhile, microplastics already accumulated in the bank soil may also be evacuated after soaking (Chen et al., 2022; Zhang et al., 2019). When the water level decreases, the buoyant microplastics may be deposited into the HFB owing to the soil–water interface effects, while the accumulated microplastics may be readily released owing to the modified hydraulic conditions (Chen et al., 2022; Zhang et al., 2019). Thus, understanding the occurrence and fate of microplastics in this sensitive area has become a research priority.

[1]State Key Laboratory of Simulation and Regulation of Water Cycle in River Basin, China Institute of Water Resources and Hydropower Research, Beijing 100038, China

[2]State Key Laboratory of Water Environment Simulation, School of Environment, Beijing Normal University, Beijing 100875, China

[3]Lead contact

*Correspondence: gaobo@iwhr.com

https://doi.org/10.1016/j.isci.2022.104401

Frequent summer floods have resulted in dramatic water level fluctuations in the HFB. Moreover, it is suspected that such fluvial flooding may be able to efficiently flush away microplastics from riparian soil into the TGR (Hurley et al., 2018; Lattin et al., 2004; Lee et al., 2013; Moore et al., 2002; Veerasingam et al., 2016), thereby introducing an extra risk of microplastics in the reservoir. Meanwhile, flooding can also drive the reorganization of local microplastics (Hurley et al., 2018). Microplastics of different polymer types, size classes, and morphologies have been found to exhibit varied accumulation and retention abilities in sediment and soil (Wang et al., 2018). On the one hand, polyethylene (PE) and polypropylene (PP) have been identified as the most produced and littered polymer types worldwide (Geyer et al., 2017) and have generally been determined to be the chief components of microplastics contamination in different environmental media (Bergmann et al., 2017; Enders et al., 2015; Erni-Cassola et al., 2019; Kanhai et al., 2017; Pabortsava and Lampitt, 2020; Peeken et al., 2018). On the other hand, the small-sized microplastics were preferentially accumulated in sediments owing to their specific characteristics and possibly explain the relative absence of small microplastics in the surface water of the ocean (Wang et al., 2018). Different from a plain river network, HFB experiences an anti-seasonal ebb and flow of water levels. The preference of different microplastics to accumulate in or be released from this unique zone (Chen et al., 2022; Woodward et al., 2021), however, is far from robust. The hypothesis is that certain polymer types may have differential susceptibility to being either retained in or released from the HFB.

In this study, we investigated the temporal and spatial distribution of microplastics in the HFB before and after catastrophic-scale flooding, based on a comprehensive analysis of polymer type, morphology, and whole-size characteristics (10–5,000 μm). This study focused on the HFB in the upstream region of the Three Gorges Dam. Four representative tributaries, Zhuyi River (ZYR), Meixi River (MXR), Daning River (DNR), and Xiangxi River (XXR), and two mainstream locations at Taipingxi (TPX) and Maoping (MP) towns were selected for microplastics detection (Figure 1A). The microplastics distribution in the upstream (*xxx*-U), midstream (*xxx*-M), and downstream (*xxx*-D) reaches of these four tributaries were investigated. Here, *xxx* represents the acronym of the aforementioned tributaries. The objectives of this study were to: 1) investigate the temporal and spatial distribution of local microplastics in riparian soil pre- and post-flooding within the HFB and estimate their potential risks; 2) investigate the flood-driven flushing and reorganization of microplastics in the HFB and determine which types of microplastics were prone to be released or retained; and 3) calculate the total amount of microplastics evacuated into the TGR after the flood event.

RESULTS AND DISCUSSIONS

Occurrence, abundance, and flood-driven evacuation of microplastics in riparian soil

Microplastics were pervasive across all sampling sites in the HFB with their number and mass concentrations varied by several orders of magnitude with coordinate and sampling time series (Figure 1). The mean microplastics abundance failed from 7,633 ± 4,036 items/kg for pre-flooding to 4,875 ± 1,722 items/kg for post-flooding (Figure 1C), suggesting an efficient evacuation of microplastics from the HFB. This can be supported by the efficient flushing of microplastics from coastal locations and river catchments by fluvial flooding (Hurley et al., 2018; Lattin et al., 2004; Lee et al., 2013; Moore et al., 2002; Veerasingam et al., 2016). Also, the increased microplastic contamination in the surface water of TGR can serve as a support of riparian soil as a source of microplastics under flooding (Xu et al., 2022).

With respect to each tributary, microplastics were significantly evacuated from ZYR, MXR, and DNR, with DNR exhibiting the highest removal of microplastics (Figure 1D). The release of microplastics in XXR, however, was not prominent. Moreover, the great mismatch in spatial distribution and evacuation at different river reaches was potentially associated with river scale and hydrological conditions. Of the 10 sampling sites in the tributaries, microplastics were significantly flushed away from eight sites, with the largest removal being 79.9% (equivalent to 11,940 items/kg) occurring at DNR-U (Figures 1B and 1C). The remaining two sites (i.e., the HFB at XXR-M and XXR-D), however, accumulated quite a bit of microplastics, which contributed to the overall insignificant evacuation of microplastics in the XXR tributary. The increasing burial of microplastics at the XXR-M and XXR-D sites can potentially be attributed to the accumulation of microplastics flushed from upstream.

After size- and morphology-specific mass conversion, the mass concentrations of microplastics were estimated to be 44 ± 41 mg/kg pre-flooding and 18 ± 7 mg/kg post-flooding (Figure 1E). Our results were smaller than previous records of 300–67,500 mg/kg in industrial soil (Fuller and Gautam, 2016). The mass concentrations of microplastics pre-flooding followed a descending order of ZYR > MXR > TPX > DNR > XXR > MP. After fluvial

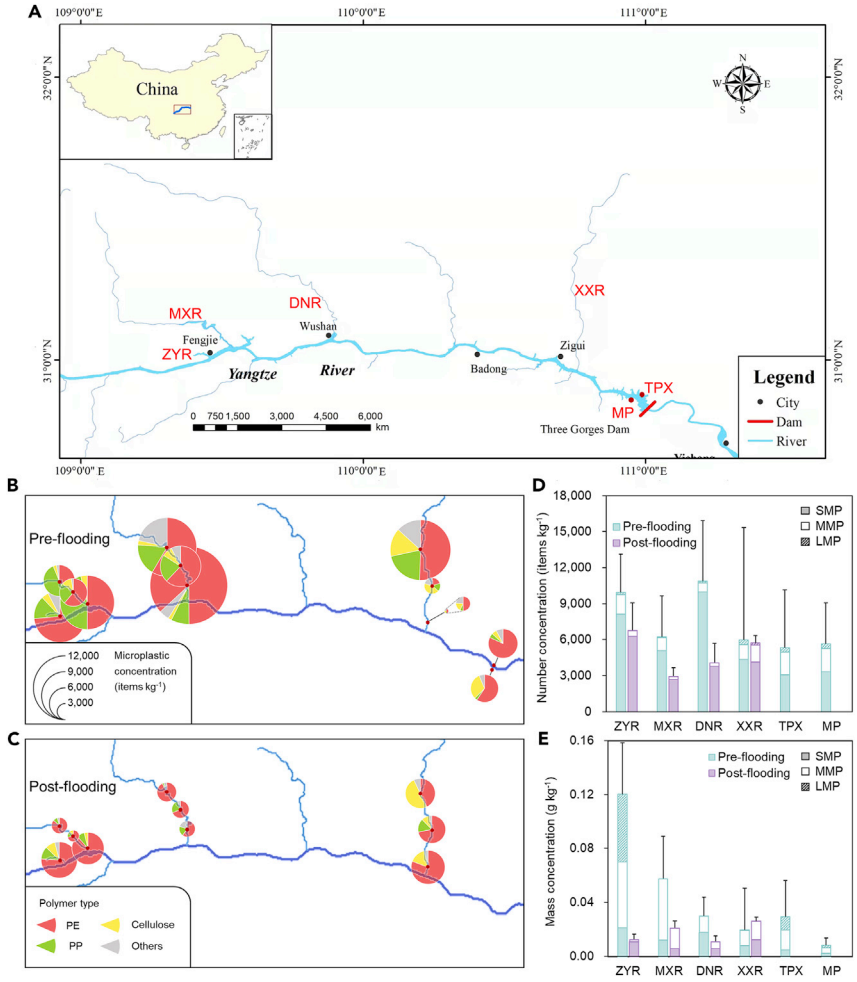

Figure 1. Microplastics abundance and constitution across 12 sites over 4 tributaries and 2 mainstream locations pre- and post-flooding

(A) Study area. The location of 4 tributaries was annotated in red words on the main map. The inset demonstrated the specific location of our study area in China.

(B and C) Microplastics abundance and polymer constitution across 12 sampling sites pre- (B) and post-flooding (C). The size of the wedge represented the relative proportion of certain polymers in the whole microplastics. The red dots represented the sampling locations.

(D and E) Number (D) and mass concentration (E) of SMP, MMP, and LMP along different rivers pre- and post-flooding. The vertical bars represented positive standard deviation of overall number and mass concentrations of microplastics.

flooding, the mass concentrations of microplastics in the tributaries significantly decreased except at XXR, which was consistent with the variation in number concentrations. The mass concentrations post-flooding followed the descending order of XXR > MXR > ZYR > DNR.

Our study also demonstrates the strong spatial heterogeneity of microplastics distribution within the HFB before flooding (Figure 2) (Chen et al., 2022). In most cases, microplastics abundance significantly decreased with increasing elevation within the HFB (Figure 2). The lower elevation sites near the water surface experienced more frequent hydraulic sorting and generally preserved higher concentrations of microplastics. One of the contributing factors to this may be that more frequent water–soil interaction provides more opportunities for microplastics to be deposited. In contrast, microplastics abundance increased with higher elevation at XXR-M and XXR-D. The varied microplastics concentration with different sampling elevations suggests that the role of the HFB switches dynamically between serving either as a source or sink for microplastics. Moreover, the role of HFB as a source or sink may be potentially affected by the hydrodynamic conditions, as well as local populations and developments along different river reaches. The

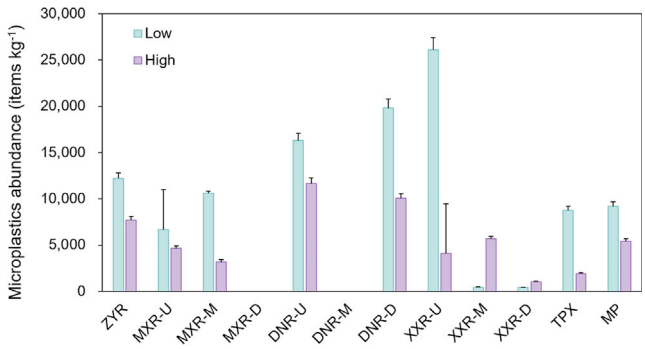

Figure 2. Spatial heterogeneity of microplastics with different elevations in HFB

Microplastics abundance at low elevation close to the surface water and high elevation of 10 m above the surface water. The two sites at MXR-D and DNR-M were not sampled at different elevations as the slope was very steep. The vertical bars represented positive standard deviation of number concentrations of microplastics.

spatial mismatch vertically and horizontally introduces serious uncertainty in identifying the severity of microplastic contaminations as well as corresponding distribution and release patterns. As such, methods of random, large-scale, and systematic sampling across different environmental media are recommended to avoid such uncertainties caused by undersampling.

Size distribution, polymer type, and morphology of microplastic in riparian soil

Overall, the microplastic contaminations in riparian soil featured a wide size range of 40–3610 μm during our two sampling campaigns. The detected microplastics were divided into three size categories: the small-sized class (<300 μm), the medium sized-class (300–1,000 μm), and the large sized-class (1,000–5,000 μm). In most cases, the small-sized microplastics dominated in number concentrations across all sampling sites, suggesting the preferential accumulation of small-sized microplastics in riparian soil (Wang et al., 2018). Recall that our pre-size division procedure facilitated the direct identification of very small particles and did not require manual sorting of suspect plastics before analysis (Kanhai et al., 2018; Peeken et al., 2018). We thus detected higher proportion of small-sized microplastics (Figure 1C) compared to previous records (Zhang et al., 2019). The mass concentrations of small-sized microplastics, however, accounted for relatively small proportions (39 $\pm$ 22%) of the total amount of detected microplastics (Figure 1D). Notably, microplastics of <1 mm dominated both in number (97 $\pm$ 3%) and mass concentration (90 $\pm$ 16%) of microplastics. Although the size class of <5 mm is most commonly applied for the definition of microplastics (Cheung and Fok, 2017; Hurley et al., 2018), our results suggest that the definition should actually be constrained to <1 mm in terms of relative proportion and toxicity considered (Jeong et al., 2016; Pabortsava and Lampitt, 2020).

In this study, a total of nine polymer types, including PE, polypropylene (PP), cellulose, polystyrene (PS), polyvinyl chloride (PVC), polyethylene terephthalate (PET), polyurethane (PU), polyacrylamide (PAM), and polyamide (PA), were identified during the two sampling campaigns (Table S1, Figure S1). In most cases, PE was the most predominant polymer type and was discovered at all sampling sites during both pre- and post-flooding (Figures 1A and 1B). Note that PE accounted for a smaller proportion than PP or cellulose at MXR-U and XXR-M before flooding and XXR-M after flooding. Moreover, PP and cellulose were less abundant but were present at most sampling sites, except that no PP was observed at XXR-U or XXR-M after flooding and no cellulose was identified at MXR-D before flooding, or at MXR-U, DNR-U, DNR-M, or DNR-D after flooding. The distribution of PS, PVC, and PET was relatively sparse (Table S1), and PU, PAM, and PA were only identified in a few subsamples. Overall, our results were consistent with the order of abundance in which polymers are littered globally (Geyer et al., 2017), and in which plastic wastes have been captured in surface water (Enders et al., 2015; Kanhai et al., 2017; Peeken et al., 2018), subsurface water (Pabortsava and Lampitt, 2020), and sediments (Bergmann et al., 2017; Erni-Cassola et al., 2019). Typically, the most littered plastics, PE and PP, are of relatively low density (0.92–0.97 and 0.88–0.91 g cm^{-1}, respectively) (Chen et al., 2021), and are supposed to transport over long distances before deposition into the ocean (Peeken et al., 2018). However, massive burial of PE and PP were observed in freshwater sediments and riparian soils prior to entering the ocean. At present, the mechanism of the preferential accumulation of low-density polymers cannot be explained with certainty. One explanation is that freshwater is of lower density, thus the vertical transport of low-density polymers is more likely to

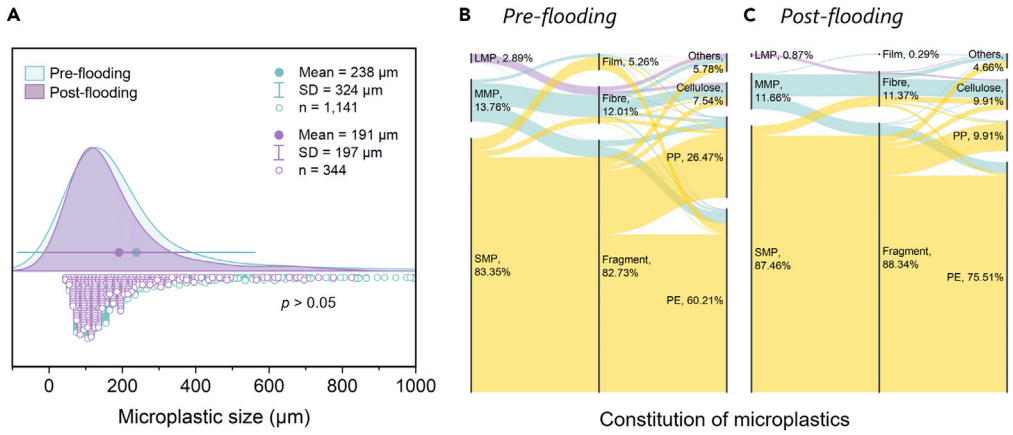

Figure 3. Flood-driven reorganization of microplastics

(A) The overall size distribution of microplastics pre- and post-flooding. The hollow circles of respective colours represented the data points that made up the size distribution. The solid dots indicated the mean particle sizes. The horizontal bars represented ± standard deviation.

(B and C) The size, morphology, and polymer constitution of microplastic pre- (B) and post-flooding (C). The flow among different characteristics indicated the comprehensive distribution of microplastics.

occur in the water column (Chen et al., 2019). Another possibility is that certain processes that facilitate the deposition of microplastics, such as biofilm colonization (Leiser et al., 2020; Lobelle et al., 2021; Miao et al., 2021; Pohl et al., 2020), suspended sediment bonding (Li et al., 2019), fecal material bonding (Cole et al., 2016), and aggregate formation (Long et al., 2015; Zhao et al., 2018), may have a preference for specific polymer type.

In most cases, the HFB featured multiple microplastics morphologies (Table S1). For example, at XXR-U before flooding, the microplastics were comprised of fragment > fiber > film, while in the midstream and downstream reaches, microplastics were mainly in the shape of fibers or films, with no observation of fragments (Table S1). In general, fragments were the most abundant and pervasive morphology with a significantly higher proportion (85.5%) compared to fibers (11.7%) and films (2.8%), suggesting the preferential accumulation of fragments in riparian soil.

Flood-induced reorganization of microplastics in riparian soil

During both the pre- and post-flooding sampling campaigns, microplastics in the HFB were characterized by similar size distribution (Figures 3A and 3B). Overall, the size of identified microplastics ranged from 40 to 3610 μm before flooding and 40 to 2330 μm after flooding, respectively. Interestingly, the flood-induced evacuation of microplastics in HFB did not significantly alter the overall size distribution, which can be supported by the minimally modified size distribution of riverine microplastics in northwest England (Hurley et al., 2018). In this study, the mean size of microplastics only slightly decreased from 238 μm before flooding to 197 μm before flooding ($p > 0.05$). Moreover, the small-sized class (<300 μm) dominated, accounting for 83.3 and 87.4% of the whole recovered microplastics pre- and post-flooding, respectively. Our findings not only provide sound evidence for the small-sized microplastics stably being a dominant component of microplastics (Enders et al., 2015; Pabortsava and Lampitt, 2020; Poulain et al., 2019; Wang et al., 2018) but also further suggest that higher proportions of small-sized microplastics can be preserved from evacuation by flooding.

Alongside the processes of flood-driven HFB scour, hydraulic sorting, and microplastic flushing, we observed a distinctive reorganization of polymer types and morphologies between pre-flooding and post-flooding. The relative proportion of different polymer types pre- and post-flooding both followed a descending order of PE > PP > cellulose (Figures 3B and 3C). However, fluvial flooding resulted in an increased proportion of PE but decreased percentage of PP in the HFB. Similarly, the post-flooding morphology constitution of microplastics revealed an increasing proportion of fragments but a decreasing proportion of both fibers and films. As such, it can be stated that PP, as well as fibers and films, may be more easily evacuated by fluvial flooding, while higher proportions of PE and fragments were preferentially retained by hydraulic sorting.

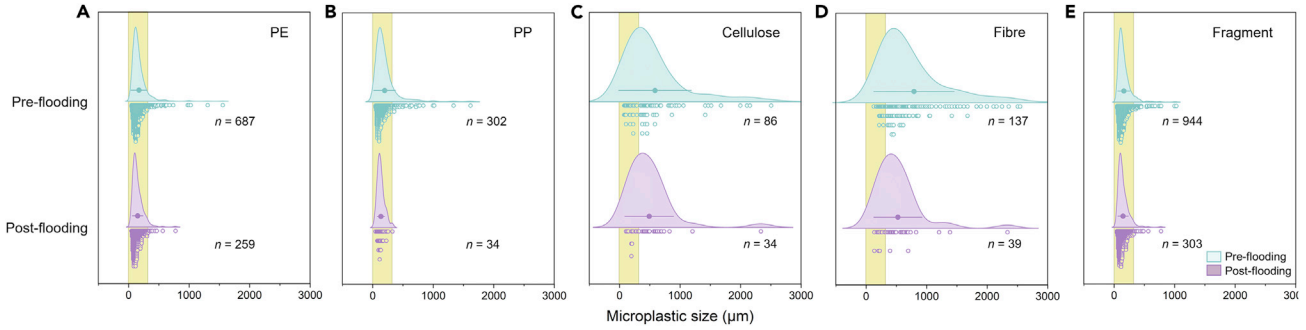

Figure 4. Size distribution of different microplastics pre- and post-flooding

(A–E) Size distribution of different polymer types (A–C) and morphology characteristics (D–E). The highlighted yellow region represented the dominance of small-sized microplastics (SMPs). The solid dots indicated the mean particle sizes. The horizontal bars represented ± standard deviation.

The flowchart further displayed a comprehensive distribution of polymer type, morphology, and dimension characteristics of microplastics pre- and post-flooding (Figures 3B and 3C). With respect to the different size classes, the small-sized microplastics were mainly comprised of fragments > fibers, films, and PE > PP > cellulose. The medium-sized microplastics were consist of fibers > fragments > films, and celluloses, PE > PP. The larger-sized microplastics mainly comprised fibers and cellulose, which can explain their relatively low contribution in mass concentrations. With respect to different morphologies, the fragment was mainly comprised of small-sized > medium-sized fractions and polymer types of PE > PP > cellulose, while fibers comprised a higher proportion of the large-sized class and cellulose (Figures 3B, 3C, and 4). As for different polymer types, PE and PP were mainly comprised small-sized fractions and fragments, while cellulose had comparable proportions of both small-sized and large-sized fractions, and was mainly characterized as fibers > fragments.

After fluvial flooding, general decreases in mean size were observed for different polymer types and morphologies (Figure 4), suggesting overall the selective preservation of the small-sized fractions. Moreover, increasing proportions of PE and fragments in the small-sized fractions were observed, while PP of both different size classes and morphologies exhibited decreasing proportions after flooding (Figures 3B and 3C). As such, the small-sized PE, which was the predominant composition of the small-sized fraction and fragments, was selectively retained by hydraulic sorting, while large amounts of PP were evacuated irrespective of size and morphology. The preferential retention of small-sized PE cannot be explained with certainty. Many processes, such as hydrodynamic sorting, biofilm colonization, microplastic degradation, heterogeneous aggregation (Besseling et al., 2017), may contribute to this phenomenon. Therefore, the influence of such processes on the preferential retention of a certain size class (Besseling et al., 2017; Wang et al., 2018), polymer type, or morphology of microplastics in soil should be further investigated.

Estimation of microplastics evacuated into the reservoir

As aforementioned, fluvial flooding caused a sharp decrease in local microplastics concentration in riparian soil. To evaluate the amount of microplastics evacuated into the reservoir, we established a novel method to estimate the quantity and mass of microplastics flushed into the reservoir. Assuming that microplastics transport with the erosion of riparian soil by flooding, the eroded riparian soil and microplastics may either redeposit to a lower elevation of the HFB or enter the water or sediment of the TGR. Thus, the amount of microplastics evacuated into the reservoir was estimated by multiplying the reduced microplastics concentration by flooding with the soil erosion amount and sediment delivery ratio (*SDR*). The soil erosion amount was calculated using the Revised Universal Soil Loss Equation model (Ma et al., 2021). The *SDR* is calculated as the ratio of sediment input into TGR to the total soil erosion amount along the catchment. In this study, the *SDR* in 2020 was calculated to be 0.29, which was consistent with previous records (Wang et al., 2015).

With respect to each tributary, the quantity of microplastics evacuated into the TGR was estimated to be 1.17×10^{13}, 9.30×10^{13}, and 7.85×10^{11} items for MXR, DNR, and XXR, respectively (Table 1). Owing to the minimal reduction of local microplastics in XXR, the evacuated quantity of XXR was two orders of magnitude lower than that of MMR and DNR. In contrast, an ultra-high quantity of microplastics was released from DNR, which was potentially attributed to its higher soil erosion amount and greater reduction of local

Table 1. Estimation of microplastics evacuated into the reservoir bed

Study area	Soil erosion amount (million tons)	Area of HFB (m^{-2})	Quantity of MPs input into TGR (items)	Mass of MPs input into TGR (tons)
MXH	12.27	2.86×10^{9}	1.17×10^{13}	129.55
DNH	47.09	4.26×10^{9}	9.30×10^{13}	261.32
XXH	10.45	1.08×10^{9}	7.85×10^{11}	0
Whole TGR region	499.79	5.27×10^{10}	5.00×10^{14}	2683.57

microplastics concentration. After mass conversion, the mass of microplastics flushed into the TGR was estimated as 129.55, 261.32, and 0 tons in MXR, DNR, and XXR, respectively. The null value of microplastics evacuation amount from XXR was attributed to the inefficient flushing of local microplastics and the insignificant changes in microplastic mass concentration. The average quantity and mass concentrations of microplastics in eroded soil were further utilized to calculate the total microplastics input into the TGR.

Overall, the input of microplastics from riparian soil into the TGR was estimated to be 5×10^{14} items (~2,684 tons). Comparatively, this value is equivalent to 15.8 wt% of the plastic flux of the Yangtze River (17,000 tons $year^{-1}$) into the ocean (Mai et al., 2020) and 0.0073‰ of global plastic production (368 million tons in 2019) (PlasticEurope, 2020). As such, we conclude that riparian soil in the HFB is a potential source of microplastics, especially after a catastrophic flooding event.

Risk evaluation and environmental implications

Both the chemical constitution and concentration of microplastics were taken into consideration to evaluate the ecological risks of microplastic contamination in riparian soil (Figures 5A and 5B). The polymer risk index (H) demonstrated that most sites belonged to the chemical risk categories I and II, while DNR-M, XXR-M, XXR-D, and TPX before flooding, as well as DNR-D and XXR-U after flooding ranked as risk level III (Figure 5A). The ultra-high risk level at certain sites was attributed to the existence of certain polymer types of high hazard scores, such as PVC and PU (Lithner et al., 2011). Fluvial flooding profoundly altered the polymer risks of local microplastics contamination. For ZYR, MXR, DNR-D, and XXR-M, the polymer risks increased after flooding, potentially attributed to the decreasing proportion of PP (S_{PP} = 1) yet with increasing proportions of PE (S_{PE} = 11) and other high-score polymers. In contrast, the polymer risks at DNR-U, DNR-M, XXR-M, and XXR-D were significantly reduced, which was mainly attributed to the detection of PVC in soil samples collected pre-flooding. The *pollution load index (PLI)* suggested that all the sampling sites belonged to risk category I (Figure 5B and Table 2). Most sites featured higher *PLI* values pre-flooding than post-flooding, except for XXR-M and XXR-D, which was consistent with the concentration variation by flooding (Figures 1A and 1B). The PLI_{zone} of the study area (excluding two mainstream sites, TPX and MP) pre- and post-flooding was calculated as 3.9 and 3.2, respectively. These results suggest an efficient reduction of *PLI* risk by flooding.

Owing to the lack of microplastic-related health data and the huge uncertainties in the microplastics exposure level in different media, no consensus has yet been reached on an efficient method to evaluate the potential risks of microplastics. The commonly used polymer risk assessment currently does not consider the local microplastic concentration. Meanwhile, the adopted hazard score is based merely on one study about plastic products (Lithner et al., 2011), the characteristics and behavior of which may be significantly different from that of micro-scale particles, as the size and morphology of microplastics contribute to the toxicity. Moreover, the *PLI* risk level is usually incomparable among different studies, owing to the lack of background values (Xu et al., 2018). That method is somewhat simplistic, as it is based only on the local concentration of microplastics without the consideration of polymer-based hazards. With respect to the evacuated microplastics, their contribution to the risks in TGR is still unknown. Thus, it is still a challenge to judge the potential risks of local microplastics contamination, as well as that of evacuated microplastics. The implementation of coherent sampling campaigns and establishment of risk assessment methods should be focused on in upcoming research.

CONCLUSIONS

This study demonstrated the temporal and spatial variation of microplastics in TGR riparian soil, and first identified a selective evacuation phenomenon of microplastics by catastrophic fluvial flooding. During

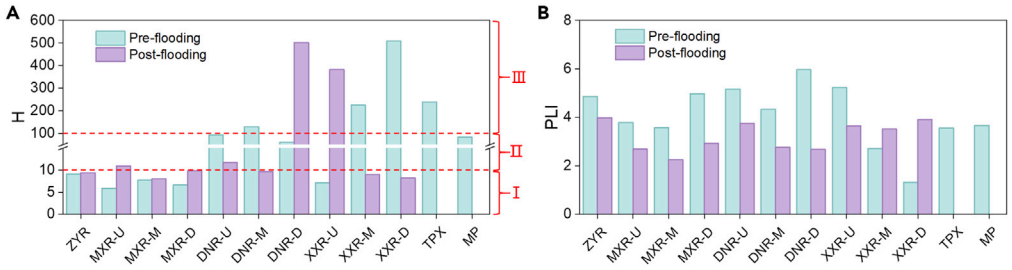

Figure 5. Ecological risks of microplastic contamination in riparian soil

(A and B) Polymer risk index "*H*" (A) and pollution load index "PLI" (B) of microplastics across 12 sites pre- and post-flooding. The red roman numerals (I, II, and III) represent the risk level according to Table 1.

two sampling campaigns pre-flooding and post-flooding, we observed ubiquitous but heterogeneous presence of microplastics across all sampling sites. It was found that the microplastics concentration within the HFB decreased at higher elevations and varied with soil characteristics. The predominance of PE, which mainly occurred as small-sized classes and fragments, was observed at most locations. Fluvial flooding efficiently decreased the microplastics abundance in the HFB, with a sharp removal of PP irrespective of its size and morphology. In contrast, the small-sized PE, which dominated the small-sized microplastics and fragments, was preferentially retained. The overall size distribution of microplastics was minimally changed by fluvial flooding, with an insignificant decrease in the mean size of the overall, polymer-, and morphology-specific microplastics. Approximately 5×10^{14} items (~2,360 tons) of microplastics were flushed into the TGR between the sampling dates, suggesting that riparian soil in the HFB is a significant source of microplastics. The flooding greatly reduced the *PLI* risk of local microplastics in the riparian soil but added to the potential risk of microplastics in the TGR. This is because, once microplastics are flushed into the TGR, they may either stay suspended in the water column or be deposited into the bottom sediment, increasing microplastic pollution in water bodies and adding to the uncertainty in evaluating the potential risk. The *in situ* remediation of microplastics in riparian soil seems necessary to avoid their emission into the reservoir.

Plastic products are still likely to be widely produced and used for ages to come owing to their currently incomparable strengths. Thus, quantifying this material in terms of its sources, sinks, and the processes responsible should be a research priority. To achieve this, highly systematic investigations should be carried out that comprehensively consider the size class, polymer type, and morphology. Meanwhile, it can be expected that the microplastic definition covering the <5 mm size class may encounter updates owing to the relatively lower proportion and toxicity of larger particles. Finally, the establishment of risk assessment methods for microplastics is recommended.

Limitations of the study

In this study, we have discussed the impact of flooding on the organization of microplastics in riparian soil. It is noteworthy that there are still several limitations needing to be addressed in future work. First, we only estimated the evacuated amount of microplastics from riparian soil to water in TGR based on the concentration decrease in riparian soil rather than continuously monitoring the variation of microplastic concentration in the water of different layers. Thus, the fate of microplastics in riparian soil still remains unclear. The evacuation of riparian microplastics in this study and the increased microplastic contamination in surface water according to our previous work (Xu et al., 2022) can partly serve as an evidence of riparian soil as a source. However, the switching role of riparian soil as a source or sink still merits further investigations. Second, the preferential accumulation and evacuation phenomenon needs further verification whether it

Table 2. Classification of microplastics risk levels

Risk level	H	PLI
I	<10	<10
II	10–100	10–100
III	100–1000	100–1000
IV	>1000	>1000

is an occasional phenomenon or a long-term rule. Last but not least, there is a dearth of information on the fragmentation and deposition mechanisms of microplastics in HFB, which are of crucial importance to help understand the occurrence and fate of microplastics.

STAR★METHODS

Detailed methods are provided in the online version of this paper and include the following:

- KEY RESOURCES TABLE
- RESOURCE AVAILABILITY
  - Lead contact
  - Materials availability
  - Data and code availability
- METHOD DETAILS
  - Study area and experimental design
  - Microplastics extraction and identification
  - Mass conversion
  - Estimation of microplastics evacuated into the reservoir
  - Risk assessment of riparian microplastics
  - Statistical analysis

SUPPLEMENTAL INFORMATION

Supplemental information can be found online at https://doi.org/10.1016/j.isci.2022.104401.

ACKNOWLEDGMENTS

This work is financially supported by the Special Fund Projects of State Key Laboratory of Simulation and Regulation of Water Cycle in River Basin, China Institute of Water Resources and Hydropower Research (SKL2020ZY02; SKL2022TS02), and the Research & Development Support Program of China Institute of Water Resources and Hydropower Research (WE0145B662021). We also thank colleagues in the State Key Laboratory of Simulation and Regulation of Water Cycle in River Basin at the China Institute of Water Resources and Hydropower Research for help with a range of field sampling and laboratory analyses.

AUTHOR CONTRIBUTIONS

Y.C. designed the study, conducted the ansalyses, and wrote the original article draft. B.G. acquired financial support, initiated the microplastics project, helped to design the study, and assisted in the preparation and revision of the article. D.X. undertook the field sampling, performed microplastic identification, and contributed to the article editing. K.S. assisted in the revision of the article. Y. L. contributed to the data interpretation.

DECLARATION OF INTERESTS

The authors declare no competing interests.

Received: January 15, 2022
Revised: April 18, 2022
Accepted: May 6, 2022
Published: June 17, 2022

REFERENCES

Alimi, O.S., Farner Budarz, J., Hernandez, L.M., and Tufenkji, N. (2018). Microplastics and nanoplastics in aquatic environments: aggregation, deposition, and enhanced contaminant transport. Environ. Sci. Technol. *52*, 1704–1724. https://doi.org/10.1021/acs.est.7b05559.

Bergmann, M., Wirzberger, V., Krumpen, T., Lorenz, C., Primpke, S., Tekman, M.B., and Gerdts, G. (2017). High quantities of microplastic in arctic deep-sea sediments from the HAUSGARTEN observatory. Environ. Sci. Technol. *51*, 11000–11010. https://doi.org/10.1021/acs.est.7b03331.

Besseling, E., Quik, J.T.K., Sun, M., and Koelmans, A.A. (2017). Fate of nano- and microplastic in freshwater systems: a modeling study. Environ. Pollut. *220*, 540–548. https://doi.org/10.1016/j.envpol.2016.10.001.

Chen, S., Li, W., Zhang, K., Xiong, W., Zhang, X., and Liu, Z. (2022). Distribution characteristics of microplastics and their migration patterns in Xiangxi River Basin. Environmental Science (China), 1–14. https://doi.org/10.13227/j.hjkx.202109268.

Chen, X., Xiong, X., Jiang, X., Shi, H., and Wu, C. (2019). Sinking of floating plastic debris caused by biofilm development in a freshwater lake. Chemosphere *222*, 856–864.

https://doi.org/10.1016/j.chemosphere.2019.02.015.

Chen, Y., Sun, K., Han, l., and Gao, B. (2021). Separation, identification, and quantification methods in soil microplastics analysis: a review. Acta Pedol. Sin. https://doi.org/10.11766/trxb202012070566.

Cheung, P.K., and Fok, L. (2017). Characterisation of plastic microbeads in facial scrubs and their estimated emissions in Mainland China. Water Res. *122*, 53–61. https://doi.org/10.1016/j.watres.2017.05.053.

Cole, M., Lindeque, P.K., Fileman, E., Clark, J., Lewis, C., Halsband, C., and Galloway, T.S. (2016). Microplastics alter the properties and sinking rates of zooplankton faecal pellets. Environ. Sci. Technol. *50*, 3239–3246. https://doi.org/10.1021/acs.est.5b05905.

Enders, K., Lenz, R., Stedmon, C.A., and Nielsen, T.G. (2015). Abundance, size and polymer composition of marine microplastics ≥10μm in the Atlantic Ocean and their modelled vertical distribution. Mar. Pollut. Bull. *100*, 70–81. https://doi.org/10.1016/j.marpolbul.2015.09.027.

Erni-Cassola, G., Zadjelovic, V., Gibson, M.I., and Christie-Oleza, J.A. (2019). Distribution of plastic polymer types in the marine environment; A meta-analysis. J. Hazard Mater. *369*, 691–698. https://doi.org/10.1016/j.jhazmat.2019.02.067.

Fuller, S., and Gautam, A. (2016). A procedure for measuring microplastics using pressurized fluid extraction. Environ. Sci. Technol. *50*, 5774–5780. https://doi.org/10.1021/acs.est.6b00816.

Geyer, R., Jambeck, J.R., and Law, K.L. (2017). Production, use, and fate of all plastics ever made. Sci. Adv. *3*, e1700782. https://doi.org/10.1126/sciadv.1700782.

Hurley, R., Woodward, J., and Rothwell, J.J. (2018). Microplastic contamination of river beds significantly reduced by catchment-wide flooding. Nat. Geosci. *11*, 251–257. https://doi.org/10.1038/s41561-018-0080-1.

Jeong, C.-B., Won, E.-J., Kang, H.-M., Lee, M.-C., Hwang, D.-S., Hwang, U.-K., Zhou, B., Souissi, S., Lee, S.-J., and Lee, J.-S. (2016). Microplastic size-dependent toxicity, oxidative stress induction, and p-JNK and p-p38 activation in the monogonont rotifer (Brachionus koreanus). Environ. Sci. Tech. *50*, 8849–8857. https://doi.org/10.1021/acs.est.6b01441.

Jin, Y., Lu, L., Tu, W., Luo, T., and Fu, Z. (2019). Impacts of polystyrene microplastic on the gut barrier, microbiota and metabolism of mice. Sci. Total Environ. *649*, 308–317. https://doi.org/10.1016/j.scitotenv.2018.08.353.

Jung, J.-W., Park, J.-W., Eo, S., Choi, J., Song, Y.K., Cho, Y., Hong, S.H., and Shim, W.J. (2021). Ecological risk assessment of microplastics in coastal, shelf, and deep sea waters with a consideration of environmentally relevant size and shape. Environ. Pollut. *270*, 116217. https://doi.org/10.1016/j.envpol.2020.116217.

Kanhai, L.D.K., Gårdfeldt, K., Lyashevska, O., Hassellöv, M., Thompson, R.C., and O'Connor, I. (2018). Microplastics in sub-surface waters of the arctic central basin. Mar. Pollut. Bull. *130*, 8–18. https://doi.org/10.1016/j.marpolbul.2018.03.011.

Kanhai, L.D.K., Officer, R., Lyashevska, O., Thompson, R.C., and O'Connor, I. (2017). Microplastic abundance, distribution and composition along a latitudinal gradient in the Atlantic Ocean. Mar. Pollut. Bull. *115*, 307–314. https://doi.org/10.1016/j.marpolbul.2016.12.025.

Koelmans, A.A., Bakir, A., Burton, G.A., and Janssen, C.R. (2016). Microplastic as a vector for chemicals in the aquatic environment: critical review and model-supported reinterpretation of empirical studies. Environ. Sci. Technol. *50*, 3315–3326. https://doi.org/10.1021/acs.est.5b06069.

Lattin, G.L., Moore, C.J., Zellers, A.F., Moore, S.L., and Weisberg, S.B. (2004). A comparison of neustonic plastic and zooplankton at different depths near the southern California shore. Mar. Pollut. Bull. *49*, 291–294. https://doi.org/10.1016/j.marpolbul.2004.01.020.

Lee, J., Hong, S., Song, Y.K., Hong, S.H., Jang, Y.C., Jang, M., Heo, N.W., Han, G.M., Lee, M.J., Kang, D., and Shim, W.J. (2013). Relationships among the abundances of plastic debris in different size classes on beaches in South Korea. Mar. Pollut. Bull. *77*, 349–354. https://doi.org/10.1016/j.marpolbul.2013.08.013.

Leiser, R., Wu, G.-M., Neu, T.R., and Wendt-Potthoff, K. (2020). Biofouling, metal sorption and aggregation are related to sinking of microplastics in a stratified reservoir. Water Res. *176*, 115748. https://doi.org/10.1016/j.watres.2020.115748.

Li, Y., Wang, X., Fu, W., Xia, X., Liu, C., Min, J., Zhang, W., and Crittenden, J.C. (2019). Interactions between nano/micro plastics and suspended sediment in water: implications on aggregation and settling. Water Res. *161*, 486–495. https://doi.org/10.1016/j.watres.2019.06.018.

Lithner, D., Larsson, Å., and Dave, G. (2011). Environmental and health hazard ranking and assessment of plastic polymers based on chemical composition. Sci. Total Environ. *409*, 3309–3324. https://doi.org/10.1016/j.scitotenv.2011.04.038.

Liu, M., Zhang, Q., Ge, S., Mason, R.P., Luo, Y., He, Y., Xie, H., Sa, R., Chen, L., and Wang, X. (2019). Rapid Increase in the Lateral Transport of Trace Elements Induced by Soil Erosion in Major Karst Regions in China. Environ. Sci. Technol. *53*, 4206–4214. https://doi.org/10.1021/acs.est.8b06143.

Lobelle, D., Kooi, M., Koelmans, A.A., Laufkötter, C., Jongedijk, C.E., Kehl, C., and van Sebille, E. (2021). Global modeled sinking characteristics of biofouled microplastic. J. Geophys. Res. Oceans *126*. e2020JC017098. https://doi.org/10.1029/2020JC017098.

Long, M., Moriceau, B., Gallinari, M., Lambert, C., Huvet, A., Raffray, J., and Soudant, P. (2015). Interactions between microplastics and phytoplankton aggregates: impact on their respective fates. Mar. Chem. *175*, 39–46. https://doi.org/10.1016/j.marchem.2015.04.003.

Ma, X., Zhao, C., and Zhu, J. (2021). Aggravated risk of soil erosion with global warming – a global meta-analysis. CATENA *200*, 105129. https://doi.org/10.1016/j.catena.2020.105129.

Mai, L., Sun, X.-F., Xia, L.-L., Bao, L.-J., Liu, L.-Y., and Zeng, E.Y. (2020). Global riverine plastic outflows. Environ. Sci. Technol. *54*, 10049–10056. https://doi.org/10.1021/acs.est.0c02273.

Masura, J., Baker, J., Foster, G., and Arthur, C. (2015). Laboratory Methods for the Analysis of Microplastics in the Marine Environment: Recommendations for Quantifying Synthetic Particles in Waters and Sediments (NOAA Technical Memorandum NOS-OR&R-48).

Miao, L., Gao, Y., Adyel, T.M., Huo, Z., Liu, Z., Wu, J., and Hou, J. (2021). Effects of biofilm colonization on the sinking of microplastics in three freshwater environments. J. Hazard Mater. *413*, 125370. https://doi.org/10.1016/j.jhazmat.2021.125370.

Moore, C.J., Moore, S.L., Weisberg, S.B., Lattin, G.L., and Zellers, A.F. (2002). A comparison of neustonic plastic and zooplankton abundance in southern California's coastal waters. Mar. Pollut. Bull. *44*, 1035–1038. https://doi.org/10.1016/S0025-326X(02)00150-9.

Nilsson, C., Reidy, C.A., Dynesius, M., and Revenga, C. (2005). Fragmentation and flow regulation of the World's large river systems. Science *308*, 405–408. https://doi.org/10.1126/science.1107887.

Niu, J., Gao, B., Wu, W., Peng, W., and Xu, D. (2022). Occurrence, stability and source identification of small size microplastics in the Jiayan reservoir, China. Sci. Total Environ. *807*, 150832. https://doi.org/10.1016/j.scitotenv.2021.150832.

Pabortsava, K., and Lampitt, R.S. (2020). High concentrations of plastic hidden beneath the surface of the Atlantic Ocean. Nat. Commun. *11*, 4073. https://doi.org/10.1038/s41467-020-17932-9.

Peeken, I., Primpke, S., Beyer, B., Gütermann, J., Katlein, C., Krumpen, T., Bergmann, M., Hehemann, L., and Gerdts, G. (2018). Arctic sea ice is an important temporal sink and means of transport for microplastic. Nat. Commun. *9*, 1505. https://doi.org/10.1038/s41467-018-03825-5.

PlasticEurope. (2020). Plastics—The Facts 2009-2020, an Analysis of European Plastics Production, Demand and Waste Data, pp. 1–42. https://plasticseurope.org/knowledge-hub/plastics-the-facts-2020/.

Pohl, F., Eggenhuisen, J.T., Kane, I.A., and Clare, M.A. (2020). Transport and burial of microplastics in deep-marine sediments by turbidity currents. Environ. Sci. Technol. *54*, 4180–4189. https://doi.org/10.1021/acs.est.9b07527.

Poulain, M., Mercier, M.J., Brach, L., Martignac, M., Routaboul, C., Perez, E., Desjean, M.C., and ter Halle, A. (2019). Small microplastics as a main contributor to plastic mass balance in the north atlantic subtropical gyre. Environ. Sci. Technol. *53*, 1157–1164. https://doi.org/10.1021/acs.est.8b05458.

Seeley, M.E., Song, B., Passie, R., and Hale, R.C. (2020). Microplastics affect sedimentary microbial communities and nitrogen cycling. Nat. Commun. *11*, 2372. https://doi.org/10.1038/s41467-020-16235-3.

Senathirajah, K., Attwood, S., Bhagwat, G., Carbery, M., Wilson, S., and Palanisami, T. (2021). Estimation of the mass of microplastics ingested – a pivotal first step towards human health risk assessment. J. Hazard Mater. *404*, 124004. https://doi.org/10.1016/j.jhazmat.2020.124004.

Veerasingam, S., Mugilarasan, M., Venkatachalapathy, R., and Vethamony, P. (2016). Influence of 2015 flood on the distribution and occurrence of microplastic pellets along the Chennai coast, India. Mar. Pollut. Bull. *109*, 196–204. https://doi.org/10.1016/j.marpolbul.2016.05.082.

Wang, D., Shao, J., Wang, J., Li, Y., Ni, J., Gao, M., and Xie, D. (2015). Estimation of sediment delivery ratio and modelling of absorbed nitrogen and phosphorus load in Three Gorges Reservoir Area nearly 20 years *31*, 167–176.

Wang, Z., Su, B., Xu, X., Di, D., Huang, H., Mei, K., Dahlgren, R.A., Zhang, M., and Shang, X. (2018). Preferential accumulation of small (<300 μm) microplastics in the sediments of a coastal plain river network in eastern China. Water Res. *144*, 393–401. https://doi.org/10.1016/j.watres.2018.07.050.

Woodward, J., Li, J., Rothwell, J., and Hurley, R. (2021). Acute riverine microplastic contamination due to avoidable releases of untreated wastewater. Nat. Sustain. *4*, 793–802. https://doi.org/10.1038/s41893-021-00718-2.

Xu, D., Gao, B., Wan, X., Peng, W., and Zhang, B. (2022). Influence of catastrophic flood on microplastics organization in surface water of the Three Gorges Reservoir, China. Water Res. *211*, 118018. https://doi.org/10.1016/j.watres.2021.118018.

Xu, P., Peng, G., Su, L., Gao, Y., Gao, L., and Li, D. (2018). Microplastic risk assessment in surface waters: a case study in the Changjiang Estuary, China. Mar. Pollut. Bull. *133*, 647–654. https://doi.org/10.1016/j.marpolbul.2018.06.020.

Zhang, K., Chen, X., Xiong, X., Ruan, Y., Zhou, H., Wu, C., and Lam, P.K.S. (2019). The hydro-fluctuation belt of the Three Gorges Reservoir: source or sink of microplastics in the water? Environ. Pollut. *248*, 279–285. https://doi.org/10.1016/j.envpol.2019.02.043.

Zhao, S., Ward, J.E., Danley, M., and Mincer, T.J. (2018). Field-based evidence for microplastic in marine aggregates and mussels: implications for trophic transfer. Environ. Sci. Technol. *52*, 11038–11048. https://doi.org/10.1021/acs.est.8b03467.

STAR★METHODS

KEY RESOURCES TABLE

REAGENT OR RESOURCE	SOURCE	IDENTIFIER
Chemicals, peptides and recombinant proteins		
$ZnCl_2$	Beijing Chemical Works	Standard No. HG3-947-76
$FeSO_4$	Damao Chemical Reagent Factory	CAS: 7782-63-0
H_2O_2	Merck KGaA	CAS: 1.07298.1000
NaCl	Sinopharm Chemical ReagentCo., Ltd	CAS: 7647-14-5
Software and algorithms		
SPSS Statistics 22.0	IBM Corporation	Chicago, USA
OriginPro 2019	OriginLab Corporation	Massachusetts, USA

RESOURCE AVAILABILITY

Lead contact

Further information and results for resources and reagents should be directed to and will be fulfilled by the lead contact, Bo Gao (gaobo@iwhr.com).

Materials availability

This study did not generate new unique materials.

Data and code availability

- All data reported in this paper will be shared by the lead contact upon request.
- This paper does not report original code.
- Any additional information required to reanalyze the data reported in this paper is available from the lead contact upon request.

METHOD DETAILS

Study area and experimental design

The first phase of riparian soil sampling was conducted pre-flooding on June 20-25, 2020. During July and August in 2020, five massive floods of >5000 $m^3 s^{-1}$ or above the warning level were discharged from the Three Gorges Dam. The peak discharge of Flood No. 5 on August 17 was over 75,000 $m^3 s^{-1}$, exceeding ever the largest flood on record of 63,300 $m^3 s^{-1}$ in 1998. After catastrophic flooding, we then carried out a repeat sampling campaign at all sites along the four selected tributaries on October 21 to 24, 2020. The two sites on the mainstream (TPX and MP) were not resampled due to the precipitous and slippery conditions after flooding. Full sampling sites and time information are provided in Table S1.

Riparian soil samples from the HFB were collected using a stainless-steel shovel. At each site, three intact soil cores were sampled randomly at an altitude of 165 m and 175 m combined homogeneously into one composite sample before flooding. Besides, the composite samples were also collected at 165 m within the HFB for comparison after flooding, in order to account for any altitude variability. Moreover, soil samples of different characteristics (i.e. adjacent agricultural lands and grassland, and distinctly different colored soils) were collected separately as different composite samples. During the two designed sampling campaigns pre- and post-flooding, a total of 42 composite soil samples were collected. The fresh soil samples were immediately transported to the laboratory using aluminum foil bags to prevent external microplastics contamination. The riparian soil samples were thoroughly mixed and freeze dried, and the impurities, such as stone and roots, were manually removed. Then, soil samples were passed through a 5-mm sieve and stored at −20°C until analysis.

Microplastics extraction and identification

Microplastics were isolated using a density separation technique according to the National Oceanic and Atmospheric Administration protocol with minor modifications (Masura et al., 2015; Niu et al., 2022). Approximately 250 mL of $ZnCl_2$ (1.6 g cm^{-3}) solution was added to 20 g soil for microplastics separation. The density separation method was performed twice for each sample to ensure complete isolation of microplastics from riparian soil. The supernatants were combined and successively passed through 48 and 10 μm stainless-steel disks via vacuum filtration. Two subsamples of microplastics with different size classes were processed separately to produce a clearer setting for the follow-up identification of very small particles. The wet peroxide oxidation method was then applied to remove organic materials using 0.05 M iron (Fe(II)) solution and 30% hydrogen peroxide. A saturated NaCl solution (1.2 g cm^{-3}) was used for further isolation of microplastics. The supernatants were then passed through silver filter paper (Milli-Q, 0.45 μm, 25 mm diameter, United States). The filter papers were transferred to a glass petri plate and freeze dried for analysis.

Based on the aforementioned size division procedure, all the suspected plastic particles of 10–5,000 μm were carefully identified using micro-Fourier transform infrared (micro-FTIR, Thermal Scientific Nicolet iN10) spectroscopy. The spectral range was set at 4,000–650 cm^{-1}, with a spectral resolution of 4 cm^{-1}. The spectra of suspected particles were compared against the reference spectra library of different polymer types and accepted as plastic particles when the hit quality exceeded 70%. The detailed size (measured as maximum diameter), morphology, and color characteristics of all detected microplastics were measured and recorded. Our method enabled the more careful detection of smaller plastics without the influence of larger particles, thus avoiding the need to manually remove suspect plastics prior to identification (Peeken et al., 2018).

The utmost precautions were conducted to prevent contamination. Unless stated otherwise, all laboratory wares were composed of non-plastic materials such as glass or stainless steel. Prior to use, all laboratory wares were rinsed thoroughly with Milli-Q water. In addition, all glassware (e.g., beakers, filtration system, glass filters, and glass dishes) were pre-combusted at 450°C for 4 h to remove organic residuals. All samples were handled under a clean airflow cabinet in an ISO-7 ultra-clean laboratory. During sample processing, the exposed surface area of containers was minimized by covering where possible with aluminum foil or glass. By using this technique, airborne particles were excluded at the utmost. Nitrile gloves and 100% cotton lab coats were worn throughout the entirety of all laboratory procedures.

To monitor the potential introduction of airborne or consumables plastic contamination, procedural blanks were also prepared. Specifically, the blank density solution and air were drawn through the clean filter. The procedural blanks were prepared in triplicate. In line with sample processing, the procedural blanks were subjected to microplastic identification to determine background contamination. A small quantity of cotton fibers was reported, but none could be verified as plastic.

Mass conversion

The mass conversion was conducted according to Jung et al. (2021), with minor modification. The mass of individual plastic particles was estimated by multiplying morphology-specific volumes with the average density of microplastics using the following equations with the assumption that the fragment, fiber, and film shapes correspond to the sphere, cylinder, and wafer, respectively:

For fragments:

$$M_{\text{fragment}} = \rho \times \frac{1}{6}\pi d^3 \quad \text{(Equation 1)}$$

For fibers:

$$M_{\text{fibre}} = \rho \times \pi r^2 \times d \quad \text{(Equation 2)}$$

For films:

$$M_{\text{film}} = \rho \times \frac{1}{4}\pi d^2 \times h \quad \text{(Equation 3)}$$

where ρ is the average density of microplastics, 0.98 g cm^{-3} (Senathirajah et al., 2021); d is the measured maximum size of microplastics based on the stereo microscope, μm; r represents the radius of the fiber and was assumed to be 10 μm as the median radius (Jung et al., 2021); h is the thickness of the film and was assumed to be equivalent the diameter of fiber (20 μm). The weighted average mass of microplastics (M_w) was calculated as:

$$M_w = \frac{\sum_1^i M_{\text{fragment}} + \sum_1^j M_{\text{fiber}} + \sum_1^k M_{\text{film}}}{i+j+k} \quad \text{(Equation 4)}$$

where i, j, and k are the counted numbers of fragments, fibers, and films, respectively.

Estimation of microplastics evacuated into the reservoir

Firstly, the average amount of annual soil erosion was calculated using the Revised Universal Soil Loss Equation (RUSLE) model (Ma et al., 2021).

$$A = R \cdot K \cdot LS \cdot C \cdot P \quad \text{(Equation 5)}$$

where A is the average amount of annual soil erosion ($t \cdot hm^{-2} \cdot a^{-1}$), R refers to the rainfall erosivity factor ($MJ \cdot mm \cdot km^{-2} \cdot h^{-1} \cdot a^{-1}$), K is the soil erodibility factor ($t \cdot h \cdot MJ^{-1} \cdot mm^{-1}$), LS is the terrain factor, C is the vegetation cover factor, and P refers to the governance factor. Determinations of parameters for RUSLE model in this study were provided in Table S2.

Secondly, the average amount of microplastic input were calculated as follows (Liu et al., 2019).

$$M = \Delta C \cdot A \cdot S \cdot T \quad \text{(Equation 6)}$$

where M is microplastic flux from riparian soil into the water body (t/a), ΔC is the reduced microplastic concentration by flooding, A is the average amount of annual soil erosion ($t \cdot hm^{-2} \cdot a^{-1}$), S is soil erosion area (km^2), and T refers to the unit conversion factor (10^{-4}).

Thirdly, the average amount of microplastics transported into the TGR were further measured by multiplying with the sediment delivery ratio (Liu et al., 2019).

$$W = M \cdot SDR \quad \text{(Equation 7)}$$

where W is microplastic input into the TGR, M is microplastic flux from riparian soil into the water body, and SDR is the sediment delivery ratio (%). The SDR is calculated as the ratio of sediment input into TGR to the total soil erosion amount along the catchment. In this study, the SDR in 2020 was calculated as 0.29, which was consistent with previous records (Wang et al., 2015).

Risk assessment of riparian microplastics

We identified nine polymer types (PE, PP, cellulose, PS, PVC, PET, PU, PAM, and PA) during the two sampling campaigns (Table S1, Figure S1). Considering the toxicity of certain polymer types, the polymer hazard scores by Lithner et al. (2011). were utilized to estimate the chemical risks of microplastics contamination. The chemical risks were calculated as follows:

$$H = \sum P_n \times S_n \quad \text{(Equation 8)}$$

where H is the polymer risk index, n refers to certain polymer, P_n is the percentage of certain polymer type, and S_n is the hazard score for each polymer according to Lithner et al. (2011) The hazard scores used in this study were categorized as: $S_{PE} = 11$, $S_{PP} = 1$, $S_{PVC} = 10{,}551$, $S_{PS} = 30$, $S_{PET} = 4$, $S_{PA} = 47$, and $S_{PU} = 7384$.

The PLI was also applied to assess the pollution degree at each sampling site (Xu et al., 2018). The PLI was calculated as follows:

$$CF_i = C_i / C_{oi} \quad \text{(Equation 9)}$$

$$PLI_i = \sqrt{CF_i} \quad \text{(Equation 10)}$$

$$PLI_{\text{zone}} = \sqrt[n]{PLI_1 PLI_2 \cdots PLI_i} \quad \text{(Equation 11)}$$

where PLI_i is the pollution load index of site i, CF_i is the quotient of the microplastics concentration at a certain site (C_i) with the background microplastics concentration of C_{oi}, and PLI_{zone} is the calculated pollution load index of the study area. Owing to the lack of literature on microplastics contamination in riparian

soil, the C_{oi} here is defined as the observed minimal concentration (420 items/kg). The chemical constitution- and concentration-based risk level criteria are presented in Table 2.

Statistical analysis

Particle characteristics (polymer type, size, morphology, and color) and metadata on sampling information (time and coordinates) are detailly compiled in Table S1. All data were processed and visualized using the software Statistical Product and Service Solutions (SPSS 22.0) and OriginLab (OriginPro 2019). A series of tests were conducted to identify whether there were significant differences ($p < 0.05$) among the characteristics of microplastics sampled pre- and post-flooding.